Controlled Carbonization Heating Rate for Enhancing CO_2 Separation Based on Single Gas Studies

Wan Nurul Huda Wan Zainal[1*], Soon Huat Tan[2], Mohd Azmier Ahmad[2]

[1] Faculty of Chemical and Process Engineering Technology, Universiti Malaysia Pahang, Lebuhraya Tun Razak, Gambang 26300, Kuantan, Pahang, Malaysia
[2] School of Chemical Engineering, Engineering Campus, Universiti Sains Malaysia, Nibong Tebal 14300, Penang, Malaysia
* Corresponding author, e-mail: wannurulhuda@ump.edu.my

Abstract

Concerns about the impact of greenhouse gas have driven the development of new separation technology to meet CO_2 emission reduction targets. Membrane-based technologies using carbon membranes that are able to separate CO_2 efficiently appears to be a competitive method. This research was focused on the development of carbon membranes derived from polymer blend of polyetherimide and polyethylene glycol to separate CO_2 rendering it suitable to be used in many applications such as landfill gas purification, CO_2 removal from natural gas or flue gas streams. Carbonization process was conducted at temperature of 923 K and 2 h of soaking time. To enhance membrane separation properties, pore structure was tailored by varying the carbonization heating rates to 1, 3, 5, and 7 K/min. The effect of carbonization heating rate on the separation performance was investigated by single gas permeabilities using CO_2, N_2, and CH_4 at room temperature. Carbonization heating rate of 1 K/min produced carbon membrane with the most CO_2/N_2 and CO_2/CH_4 selectivity of 38 and 64, respectively, with the CO_2 permeability of 211 barrer. Therefore, carbonization needs to be carried out at sufficiently slow heating rates to avoid significant loss of selectivity of the derived carbon membranes.

Keywords

CO_2, carbonization, molecular sieve, permeation, heating rate

1 Introduction

Concerns about the impact of global warming and climate change have triggered global efforts to reduce the CO_2 concentration in the atmosphere. Increasing concerns on this issue have led to numerous attempts and development of advanced technologies to solve the problem of excessive CO_2 emitted to the atmosphere. Carbon capture and storage is the most significant technology to decrease CO_2 emission to the atmosphere, and involved separation of CO_2, transportation, and storage [1]. Among the CO_2 separation technologies, membrane-based technology is one of the most promising techniques which offers many advantages such as low capital investment, high process flexibility, and easy operation as well as compact equipment [2]. Baker [3] estimated that the market scale of the membrane-based gas separation will grow from US$ 150 million in 2002 to around US$ 760 million in year 2020. It is expected that the membrane-based gas separation plays an increasingly important role in reducing the global environmental impact and operating costs.

Currently, the dominant membranes used in the industrial gas separation are polymeric membranes. The polymeric membranes are inexpensive and easier to manufacture into large-scale modules [4]. However, at high pressures and temperatures as well as in aggressive environments, polymeric membranes undergo plasticization and compaction, which dramatically reduce membrane separation capabilities and cause irreparable damaged [5]. Carbon membrane with high thermal stability and superior chemical resistance in corrosive environments has great potential to overcome the disadvantages of polymeric membranes [6]. Carbon membrane exhibits excellent separation for gas mixtures even between gases with almost similar molecular size [7]. Carbon membrane can be prepared by controlled carbonization process of the various natural and synthetic precursors such as coal [8], polyfurfuryl alcohol (PFA) [9], polyimide [10, 11], polyetherimide [12], and cellulose acetate [13]. Carbon membrane has a unique microporous structure,

which allows it to discriminate gas molecules by size and shape [14]. The pore structure of the carbon membrane can be tailored to suit the separation of the particular gas mixtures by fine-tuning the preparation steps. Several factors including precursor selection, membrane preparation, carbonization conditions, and pre-/post treatment conditions are well recognized as important factors influenced the separation performance of carbon membranes [15, 16].

Heating rate is one of the carbonization conditions that is reported to influence the structure and properties of the derived carbon membrane [14]. Carbonization process is typically carried out at heating rate ranging from 1 to 13 K/min. Suda and Haraya [17] studied the effect of carbonization heating rate on the carbon membranes derived from the Kapton polyimide. Gas permeability of the carbon membranes increased with the increase of carbonization heating rates. Moreover, studies conducted by Sazali et al. [11] and Salleh and Ismail [18] showed that carbon membranes produced at lower heating rates produced carbon membranes with better performance than those obtained at higher heating rates.

The objective of this study was to investigate the effect of carbonization heating rates towards the morphology structure, microstructure, and gas separation performance of the polyetherimide (PEI) and polyethylene glycol (PEG) blended (PEIPEG) carbon membranes. Polymer blend solution consisting of PEI and PEG was dip coated onto the porous alumina support. The high molecular weight PEG which is a thermally labile polymer was chosen to blend with PEI to increase the diffusion pathways by the increase of total pore volume [19]. The membrane was characterized by scanning electron microscopy (SEM), X-ray diffraction (XRD), elemental analyzer (EA), and single gas permeation measurement. The distribution of membrane pore size was determined using N_2 adsorption-desorption via the Horvath-Kawazoe method.

2 Experimental
2.1 Materials
PEI was purchased from Sigma-Aldrich, USA. PEG (MW 1500), N-Methyl-2-pyrrolidone (99 %), isopropanol, and polyvinyl alcohol (88 %) were obtained from Acros Organics, USA. Membrane support was prepared from α-alumina powder supplied by Sumitomo Chemicals Co. Ltd., Japan. Aluminium triisopropylate and nitric acid (65 %) were obtained from Merck, Germany, and Fisher Scientific, respectively. Purified N_2 (99.99 %), CO_2 (99.99 %), and CH_4 (99.99 %) were supplied by Wellgas Sdn. Bhd.

2.2 Preparation of carbon membranes
Disk supported carbon membrane derived from polymer blend of PEI and PEG was prepared in this study. PEI was used as a main membrane precursor due to its superior strength and chemical resistance. PEI was blended with PEG to enhance the gas permeability as well as to improve the gas separation factor of the derived carbon membranes. Preparation of the alumina support and intermediate layer were already described in previous work [19]. The polymer solution was prepared by dissolving 2 g of PEI and 0.2 g of PEG in 18 g of N-methyl-2-pyrrolidone (NMP). The mixture was stirred at 353 K for 2 h to obtain a clear yellowish solution. The polymer solution was cooled down to room temperature before depositing on a support by a single dip-coating technique. The coated-support was immersed into the polymer solution for 10 s and carbonized in a horizontal tube furnace. Prior to carbonization, the sample was stabilized in a horizontal tube furnace at 573 K for 30 min. Stabilization process was done to promote the intermolecular cross-linking of the polymer chains and provide greater stability to sustain high temperature during carbonization [20]. Carbonization process was performed at the final carbonization temperature of 923 K and 2 h of soaking time with various heating rates (1, 3, 5, and 7 K/min). Finally, the carbon membranes were cooled down naturally to room temperature. The carbonization conditions are summarized in Table 1.

2.3 Gas permeability study
Separation performance of the derived carbon membranes was analyzed by single gas permeability study of CO_2, N_2, and CH_4 with kinetic diameter of 0.330 nm, 0.364 nm, and 0.380 nm, respectively. A single gas permeability test was conducted at an ambient temperature with feed pressure set at 2 bar using bubble soap flow meter. Fig. 1 shows the schematic diagram of the experimental set-up of the single gas permeability test. The supported carbon membrane was placed in the membrane permeation cell. Before each permeability test, both sides of the membrane

Table 1 Carbonization conditions of carbon membranes

Carbon membrane	Mass ratio PEI:PEG	Carbonization heating rate (K/min)	Carbonization condition
PEIPEG-1	1:0.1	1	nitrogen
PEIPEG-3	1:0.1	3	nitrogen
PEIPEG-5	1:0.1	5	nitrogen
PEIPEG-7	1:0.1	7	nitrogen
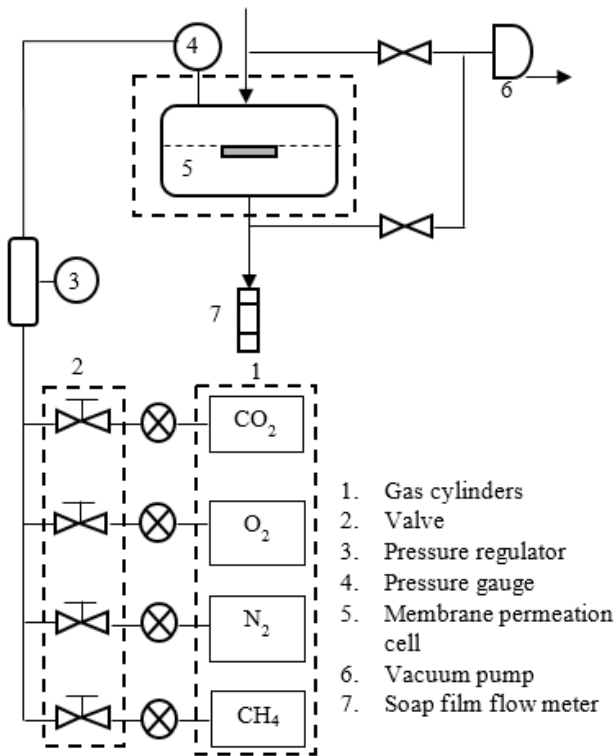
Fig. 1 Schematic diagram of the single gas permeability test set-up

1. Gas cylinders
2. Valve
3. Pressure regulator
4. Pressure gauge
5. Membrane permeation cell
6. Vacuum pump
7. Soap film flow meter

permeation cell were evacuated to less than 0.1 bar by a mechanical vacuum pump. The feed gas was introduced at the upper side of the carbon membrane.

The permeability, P of a single gas through the carbon membrane was calculated using Eq. (1):

$$P = \frac{Ql}{\Delta pA}, \tag{1}$$

where P is the permeability (cm^3(STP) cm/cm^2 s cm Hg or barrer), Q is the volumetric flow rate of gas at standard temperature and pressure (cm^3/s), l is the thickness of the membrane material (cm), Δp is the pressure difference across the membrane (cm Hg), and A is the membrane area (cm^2). The volumetric flowrate, Q of the permeate gas was calculated using Eq. (2):

$$Q = \frac{V}{t}, \tag{2}$$

where V is the volume of permeate gas (cm^3) and t is the time (s). The pressure difference between the feed side and permeate side was kept constant. After the permeability value of each gas was obtained, the ideal selectivity, α, was calculated. The ideal selectivity for pure gas A to B, $\alpha_{A/B}$ is defined as the ratio of the pure gas permeability of A, P_A toward the pure gas permeability of B, P_B and expressed in Eq. (3):

$$\alpha_{A/B} = \frac{P_A}{P_B}. \tag{3}$$

2.4 Membrane characterization

Surface and cross sectional morphologies of the carbon membrane were observed using scanning electron microscope (SEM) model Quanta FEG 450. Elemental analysis of the PEIPEG membrane before and after carbonization were determined using Perkin Elmer elemental analyzer model Series CHNS/O Analyzer 2400. X-ray powder diffraction (XRD) analysis of the carbon membrane was carried out using Philips X-ray diffractometer model PW 1820 with the $2q$ diffraction angle of 10-60° operated using Cu Ka radiation of 0.154 nm wavelength. The d-spacing value can be calculated from Bragg equation as expressed in Eq. (4):

$$n\lambda = 2d\sin\theta, \tag{4}$$

where λ is the X-ray wavelength in nm, d is the dimension spacing in nm, θ is the diffraction angle (°), and n is an order that is equal to 1. Brunauer-Emmett-Teller (BET) surface area and pore size distribution of the carbon membrane was determined using Autosorb-1C (Quantachrome Instruments) at 77 K.

3 Results and discussion
3.1 Surface morphology

SEM images of the top view and cross-sectional view of the carbon membranes derived at various carbonization heating rates are shown in Fig. 2 and Fig. 3, respectively. The top view images show that all the derived carbon membranes have a smooth and almost defect-free surface. The cross-sectional views show a three-layer structure of the carbon membranes consisting of carbon layer (top layer), Al_2O_3 intermediate layer, and alumina support (bottom layer). In this study, the Al_2O_3 intermediate layer acted as a bridge of the pore size differences between the alumina support and carbon layer. The intermediate layer acted to prevent the polymer solution from slipping into the support during coating process and it facilitated the formation of carbon layer on it. Fig. 3 shows that the carbon layer was uniformly formed on the Al_2O_3 intermediate layer. The effect of the carbonization heating rate can be seen on the thickness of the carbon layer. As the carbonization heating rates were varied to 1, 3, 5, and 7 K/min, it produced carbon membrane with carbon layer's thickness of 2.87 mm, 2.97 mm, 2.98 mm, and 3.02 mm, respectively. The higher the carbonization heating rate, the faster the time taken to reach the final carbonization temperature. Therefore, the shorter the heating duration applied, the less the effect
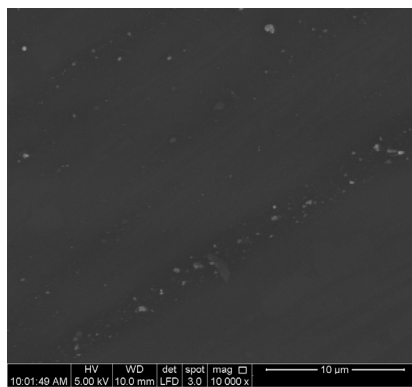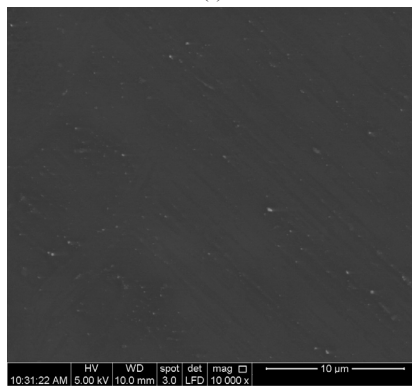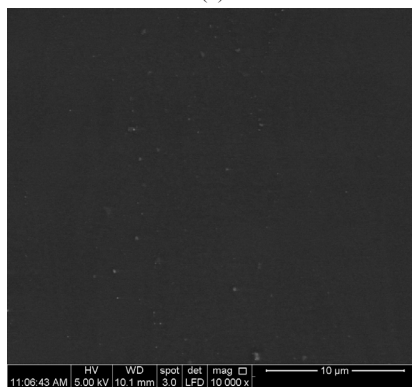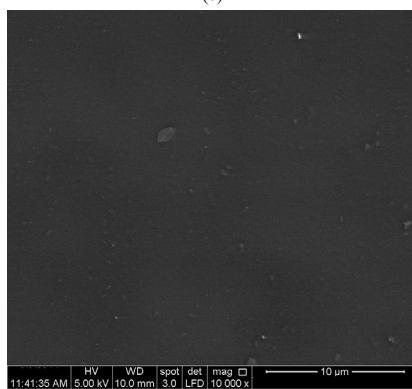
Fig. 2 Top view micrographs of PEIPEG carbon membranes carbonized at (a) 1 K/min, (b) 3 K/min, (c) 5 K/min, and (d) 7 K/min with scale bar of 10 mm and 10,000× magnification
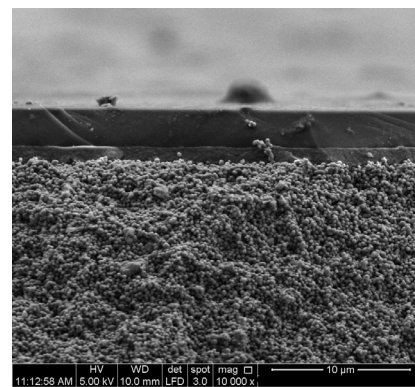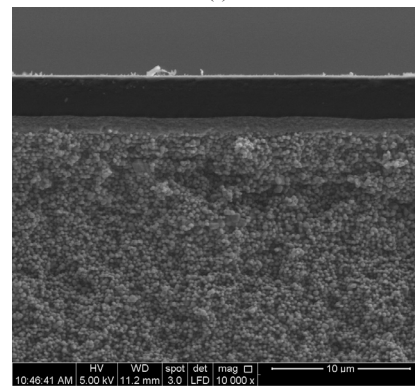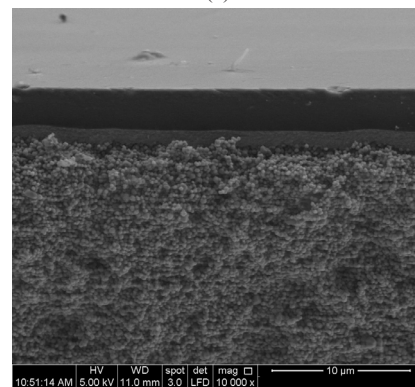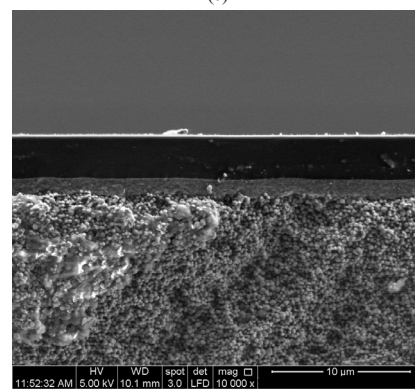
Fig. 3 Cross-sectional view micrographs of PEIPEG carbon membranes carbonized at (a) 1 K/min, (b) 3 K/min, (c) 5 K/min, and (d) 7 K/min with scale bar of 10 mm and 10,000× magnification

of thermal shrinkage on the carbon layer. It is believed that heat treatment process will affect physical structure arrangement of the membrane [11].

3.2 Microstructure analysis

In this study, XRD was used to analyze the microstructure and determine the interlayer distance (*d*-spacing) of the derived carbon membranes. The average *d*-spacing calculated using the Bragg equation does not represent the pore dimensions, but gives a measure of the distance between neighboring plane interlayer. This interlayer distance can be considered as a diffusional pathway for gas molecules through the carbon membranes [21, 22]. Fig. 4 illustrates the XRD pattern of carbon membranes derived from various carbonization heating rates. All patterns showed broad peaks which indicated the amorphous structure of the carbon membranes. Peaks were observed at $2q = 20°$ to $25°$ and another weak peak at $2q = 42°$ to $45°$ was attributed to (002) peak and (100) peak, respectively [23]. The (002) peak is derived from spacing between graphite sheets and (100) peak is related to the distance between carbon atoms within a graphite sheet [24]. As the carbonization heating rates increased from 1 to 7 K/min, the (002) peak shifted to smaller 2θ which resulted in higher *d*-spacing value. The (002) peak of the PEIPEG-1, PEIPEG-3, PEIPEG-5, and PEIPEG-7 were observed at $2\theta = 23.91°$ (*d*-spacing = 0.372 nm), $2\theta = 22.58°$ (*d*-spacing = 0.393 nm), $2\theta = 21.88°$ (*d*-spacing = 0.406 nm), and $2\theta = 21.21°$ (*d*-spacing = 0.418 nm), respectively. Based on the observation, the PEIPEG-1 showed the nearest *d*-spacing value to pure graphite (0.3354 nm). Furthermore, the (100) peak in all patterns was observed at $2q = 42° − 45°$ with *d*-spacing value of about 0.20 nm. The XRD result showed that the carbon membrane derived at 1 K/min possessed the smallest *d*-spacing and the *d*-spacing value
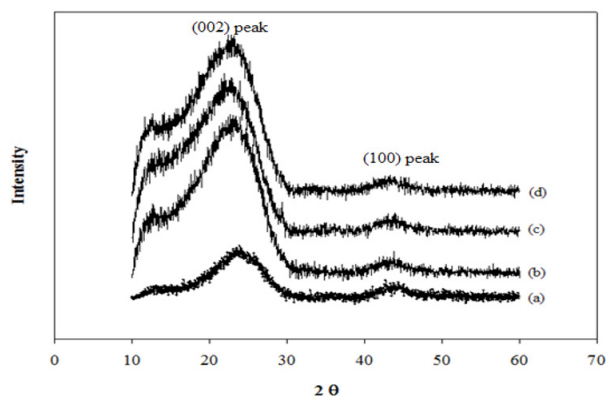
increased with the increase of heating rate. At low heating rate, the carbonization process occurred slowly. The pressure built up from the process was small and thus produced carbon membrane with more ordered structure. At high carbonization heating rate, the process occurred rapidly and had caused imperfect alignment of graphitic structures and led to higher *d*-spacing.

3.3 Elemental analysis

Table 2 summarizes percentage of elements contained in the PEIPEG precursor and PEIPEG-1 carbon membrane. After carbonization, the carbon element (C) in the PEIPEG carbon membrane increased about 9 % whereas the hydrogen (H), nitrogen (N), and oxygen (O) elements decreased about 1 - 6 %. The H/C, N/C, and O/C ratios also decreased after carbonization. During carbonization, most of the heteroatoms in the polymer precursor are volatilized in the form of methane, hydrogen, hydrogen cyanide, water, carbon monoxide, carbon dioxide, ammonia, and various other gases [25]. The evolution of gas left behind a stiff and cross-linked carbon matrix [26]. Results showed that the PEIPEG precursor had evolved to higher carbon content material after carbonization process. The observed trend was similar to the PBI/PI carbon membrane reported by Hosseini and Chung [27], in which the C content was increased, while O and N contents were decreased after carbonization as compared to its precursor.

3.4 Pore size distribution

The N_2 adsorption-desorption exhibited that the PEIPEG-1 carbon membrane has S_{BET} of 544.07 m^2/g as reported in our previous study [19]. The PEIPEG-1 carbon membrane was further analyzed to investigate the pore size distribution (PSD). The PSD of the PEIPEG-1 carbon membrane as displayed in Fig. 5 was dispersed in the range of 0.3725 to 0.9125 nm and the peak of PSD centered at about 0.7975 nm. This indicated that the PEIPEG-1 carbon membrane was comprised of bimodal structure, which consists of micropores (< 2 nm) and ultramicropores (< 0.7 nm) [28].

Fig. 4 XRD pattern of (a) PEIPEG-1, (b) PEIPEG-3, (c) PEIPEG-5, and (d) PEIPEG-7

Table 2 Results of the elemental analysis of the PEIPEG precursor and carbon membrane (CM)

Sample	Element				Ratio		
	C	H	N	^{a}O	H/C	N/C	O/C
PEIPEG precursor	67.5	7.1	5.7	19.7	0.11	0.08	0.29
PEIPEG-1 CM	76.5	6.0	4.7	12.8	0.08	0.06	0.17

^{a} Calculated by difference
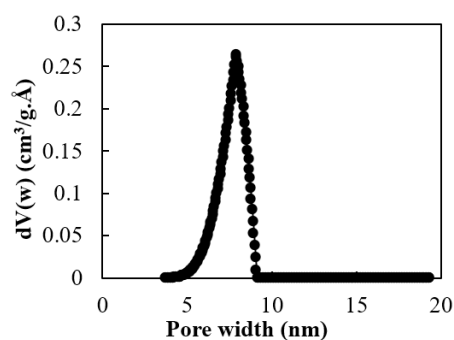
Fig. 5 PSD of the PEIPEG-1 carbon membrane estimated from the Horvath-Kawazoe method

These micropores and ultramicropores were created from imperfections between the microcrystalline regions of the polymeric material that are formed during the carbonization process [29]. The micropores contributed to the gas diffusion whereas the ultramicropores functioned for molecular sieving, which contributed to a highly permeable and highly selective carbon membrane [10]. A similar observation was obtained by carbon molecular sieve membranes prepared from novolac resin and boehmite [14].

3.5 Permeation properties
The gas permeabilities and ideal selectivities of the derived carbon membranes are tabulated in Table 3. As the carbonization heating rate increased from 1 to 3 K/min, the CO_2, N_2, and CH_4 permeabilites of the PEIPEG-1 and PEIPEG-3 were decreased by 84 %, 81 %, and 80 %, respectively. Reduction of the gas permeabilities were due to narrowing of the pore size distribution to smaller size with simultaneous densification of the carbon structure [18]. The gas permeabilities of both the PEIPEG-1 and PEIPEG-3 were in the order of $CO_2 > N_2 > CH_4$, which indicated that the gas transport through the carbon membranes was controlled by a molecular sieving.

Further increase in the carbonization heating rates to 5 and 7 K/min resulted in a significant increase of the gas permeabilities. Gas permeabilities of the PEGPEI-5 and PEGPEI-7 were in the order of $CO_2 > CH_4 > N_2$ indicating that the gas

transport neither follows molecular sieving nor Knudsen diffusion. This behavior showed that the pores structure was irregular. At low heating rate, the development of pores was uniform because pressure built up from the release of volatiles was small. There was sufficient time for the volatiles to escape through the small pores to the surface before pressure can be built up [30]. On the other hand, at higher heating rate, irregular pores formed due to the excessive increase of pressure as a result of the accumulation of evolved gases in the carbon membranes [9].

The increase of carbonization heating rate from 1 to 7 K/min reduced the carbon membrane selectivities. Carbon membranes derived at carbonization heating rates of 1 and 3 K/min exhibited relatively high ideal selectivity compared to the carbon membranes derived at 5 and 7 K/min. The highest of the CO_2/CH_4 and CO_2/N_2 ideal selectivities were achieved by the PEIPEG-1 and determined to be 64 and 38, respectively. Low carbonization heating rate led to a mild release of the volatile compounds from the matrix and produced a uniform pore structure with small pore size in the carbon matrix [9]. Subsequently, the carbon membrane produced at low carbonization heating rate became more selective. However, further increase the carbonization heating rates to 5 and 7 K/min has reduced the ideal selectivities. The loss of the ideal selectivities were possibly due to the presence of larger pores in the membranes structure. As a whole, the PEIPEG carbon membranes produced at lower carbonization heating rates showed higher ideal selectivity compared to those derived at higher carbonization heating rates. The result is in good agreement with Suda and Haraya [17].

Fig. 6 represents the trade-off between the CO_2 permeability versus the CO_2/CH_4, and CO_2/N_2 ideal selectivities of the PEIPEG carbon membranes derived at various carbonization heating rates together with the Robeson upper bound [31]. The PEIPEG-1 has exceeded the upper bound for the CO_2/CH_4 separation. For the CO_2/N_2 separation, the PEIPEG-1 nearly approached the upper bound line. This behavior shows a potential of PEIPEG carbon membranes for gas separation application.

4 Conclusion
Four different PEIPEG carbon membranes were successfully derived by carbonization of polymer blend precursors of PEI and PEG at final carbonization temperature of 923 K and 2 h of soaking time. Characterization analysis showed that the morphology and microstructure of the derived PEIPEG carbon membranes were affected

Table 3 Gas permeability and ideal selectivity of the PEIPEG carbon membranes

Carbon membrane	Gas permeability (barrer)			Ideal selectivity	
	CO_2	N_2	CH_4	CO_2/N_2	CO_2/CH_4
PEIPEG-1	211	5.60	3.30	38	64
PEIPEG-3	34	1.07	0.67	32	51
PEIPEG-5	510	172	241	2.97	2.12
PEIPEG-7	909	309	420	2.94	2.16
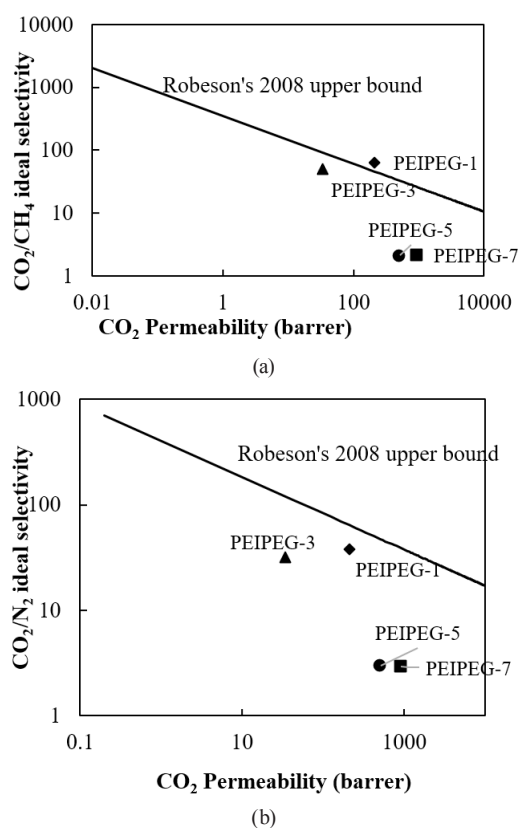
Fig. 6 Trade-off relationship between (a) CO_2 permeability and CO_2/CH_4 ideal selectivity and (b) CO_2 permeability and CO_2/N_2 ideal selectivity of the PEIPEG carbon membranes derived at various carbonization heating rates

by the carbonization heating rates. The PEIPEG carbon membranes derived at 1 K/min showed the highest of CO_2/CH_4 and CO_2/N_2 ideal selectivity, which were found to be 64 and 38 with CO_2 permeability of 211 barrer, respectively. From the study, it can be concluded that the carbonization process must be conducted at a sufficiently slow heating rate to avoid the formation of defects, which can cause a significant loss of the selectivity of the derived PEIPEG carbon membranes. The derived PEIPEG carbon membranes showed great potential to separate CO_2, rendering it suitable to be used in many applications such as CO_2 removal from natural gas or flue gas streams. As a whole, this study shows that the carbon membrane structure can be engineered by controlling the carbonization parameters depending on its applications in the industry.

Acknowledgement

References

[1] Songolzadeh, M., Soleimani, M., Ravanchi, M. T., Songolzadeh, R. "Carbon Dioxide Separation from Flue Gases: A Technological Review Emphasizing Reduction in Greenhouse Gas Emissions", The Scientific World Journal, 2014, Article ID 828131, 2014.
https://doi.org/10.1155/2014/828131

[2] Abedini, R., Nezhadmoghadam, A. "Application of membrane in gas separation processes: its suitability and mechanisms" Petroleum and Coal, 52(2), pp. 69–80, 2010.

[3] Baker, R. W. "Future Directions of Membrane Gas Separation Technology", Industrial & Engineering Chemistry Research, 41(6), pp. 1393–1411, 2002.
https://doi.org/10.1021/ie0108088

[4] Rezakazemi, M., Sadrzadeh, M., Matsuura, T. "Thermally stable polymers for advanced high-performance gas separation membranes", Progress in Energy and Combustion Science, 66, pp. 1–41, 2018.
https://doi.org/10.1016/j.pecs.2017.11.002

[5] Tin, P. S., Chung, T. S., Liu, Y., Wang, R. "Separation of CO_2/CH_4 through carbon molecular sieve membranes derived from P84 polyimide", Carbon, 42, pp. 3123–3131, 2004.
https://doi.org/10.1016/j.carbon.2004.07.026

[6] Xu, L., Rungta, M., Hessler, J., Qiu, W., Brayden, M., Martinez, M., Barbay, G., Koros, W. J. "Physical aging in carbon molecular sieve membranes", Carbon, 80, pp. 155–166, 2014.
https://doi.org/10.1016/j.carbon.2014.08.051

[7] Salleh, W. N. W., Ismail, A. F. "Carbon membranes for gas separation processes: Recent progress and future perspective", Journal of Membrane Science and Research, 1(1), pp. 2–15, 2015.
https://doi.org/10.22079/jmsr.2015.12301

[8] Liang, C., Sha, G., Guo, S. "Carbon membrane for gas separation derived from coal tar pitch", Carbon, 37(9), pp. 1391–1397, 1999.
https://doi.org/10.1016/S0008-6223(98)00334-0

[9] Song, C., Wang, T., Wang, X., Qiu, J., Cao, Y. "Preparation and gas separation properties of poly(furfuryl alcohol)-based C/CMS composite membranes", Separation and Purification Technology, 58(3), pp. 412–418, 2008.
https://doi.org/10.1016/j.seppur.2007.05.019

[10] Kim, S. J., Park, Y. I., Nam, S. E., Park, H., Lee, P. S. "Separations of F-gases from nitrogen through thin carbon membranes", Separation and Purification Technology, 158, pp. 108–114, 2016.
https://doi.org/10.1016/j.seppur.2015.12.014

[11] Sazali, N., Salleh, W. N. W., Ismail, A. F., Kadirgama, K., Othman, F. E. C., Ismail, N. H. "Impact of stabilization environment and heating rates on P84 co-polyimide/nanocrystalline cellulose carbon membrane for hydrogen enrichment", International Journal of Hydrogen Energy, 44(37), pp. 20924–20932, 2019.
https://doi.org/10.1016/j.ijhydene.2018.06.039

[12] Hamm, J. B. S., Muniz, A. R., Pollo, L. D., Marcilio, N. R., Tessaro, I. C. "Experimental and computational analysis of carbon molecular sieve membrane formation upon polyetherimide pyrolysis", Carbon, 119, pp. 21–29, 2017.
https://doi.org/10.1016/j.carbon.2017.04.011

[13] Haider, S., Linbråthen, A., Lie, J. A., Hägg, M. B. "Regenerated cellulose based carbon membranes for CO_2 separation: Durability and aging under miscellaneous environments", Journal of Industrial and Engineering Chemistry, 70, pp. 363–371, 2019.
https://doi.org/10.1016/j.jiec.2018.10.037

[14] Tanco, M. A. L., Pacheco Tanaka, D. A., Rodrigues, S. C., Texeira, M., Mendes, A. "Composite-alumina-carbon molecular sieve membranes prepared from novolac resin and boehmite. Part I: Preparation, characterization and gas permeation studies", International Journal of Hydrogen Energy, 40(16), pp. 5653–5663, 2015.
https://doi.org/10.1016/j.ijhydene.2015.02.112

[15] Favvas, E. P., Heliopoulus, N. S., Papageorgiou, S. K., Mitropoulos, A. C., Kapantaidakis, G. C., Kanellopoulos, N. K. "Helium and hydrogen selective carbon hollow fiber membranes: the effect of pyrolysis isothermal time", Separation and Purification Technology, 142, pp. 176–181, 2015.
https://doi.org/10.1016/j.seppur.2014.12.048

[16] Haider, S., Linbråthen, A., Lie, J. A., Andersen, I. C. T., Hägg, M. B. "CO_2 separation with carbon membranes in high pressure and elevated temperature applications", Separation and Purification Technology, 190, pp. 177–189, 2018.
https://doi.org/10.1016/j.seppur.2017.08.038

[17] Suda, H., Haraya, K. "Gas Permeation through Micropores of Carbon Molecular Sieve Membranes Derived from Kapton Polyimide", The Journal of Physical Chemistry, 101(20), pp. 3988–3994, 1997.
https://doi.org/10.1021/jp963997u

[18] Salleh, W. N. W., Ismail, A. F. "Effects of carbonization heating rate on CO_2 separation of derived carbon membranes", Separation and Purification Technology, 88, pp. 174–183, 2012.
https://doi.org/10.1016/j.seppur.2011.12.019

[19] Zainal, W. N. H. W., Ahmad, M. A., Tan, S. H. "Carbon Membranes Prepared from a Polymer Blend of Polyethylene Glycol and Polyetherimide", Chemical Engineering and Technology, 40(1), pp. 94–102, 2017.
https://doi.org/10.1002/ceat.201500752

[20] Yoshimune, M., Haraya, K. "Microporous Carbon Membranes", In: Membranes for Membrane Reactors: Preparation, Optimization and Selection, John Wiley & Sons, Ltd., Singapore, 2011, pp. 63–97.
https://doi.org/10.1002/9780470977569.ch1

[21] Kim, Y. K., Park, H. B., Lee, Y. M. "Gas separation properties of carbon molecular sieve membranes derived from polyimide/polyvinylpyrrolidone blends: effect of the molecular weight of polyvinylpyrrolidone", Journal of Membrane Science, 251(1-2), pp. 159–167, 2005.
https://doi.org/10.1016/j.memsci.2004.11.011

[22] Yoshimune, M., Fujiwara, I., Haraya, K. "Carbon molecular sieve membranes derived from trimethylsilyl substituted poly(phenylene oxide) for gas separation", Carbon, 45(3), pp. 553–560, 2007.
https://doi.org/10.1016/j.carbon.2006.10.017

[23] Zhang, B., Wu, Y., Wang, T., Qiu, J., Zhang, S. "Microporous carbon membranes from sulfonated poly(phthalazinone ether sulfone ketone): Preparation, characterization, and gas permeation", Journal of Applied Polymer Science, 122(2), pp. 1190–1197, 2011.
https://doi.org/10.1002/app.34261

[24] Mariwala, R. K., Foley, H. C. "Evolution of Ultramicroporous Adsorptive Structure in Poly(furfuryl alcohol)-Derived Carbogenic Molecular Sieves", Industrial & Engineering Chemistry Research, 33(3), pp. 607–615, 1994.
https://doi.org/10.1021/ie00027a018

[25] Edie, D. D. "The effect of processing on the structure and properties of carbon fibers", Carbon, 36(4), pp. 345–362, 1998.
https://doi.org/10.1016/S0008-6223(97)00185-1

[26] Salleh, W. N. W., Ismail, A. F. "Preparation of Carbon Membranes for Gas Separation", In: Comprehensive Membrane Science and Engineering, Elsevier, United Kingdom, 2017, pp. 330–357.
https://doi.org/10.1016/B978-0-12-409547-2.12241-3

[27] Hosseini, S. S., Chung, T. S. "Carbon membranes from blends of PBI and polyimides for N_2/CH_4 and CO_2/CH_4 separation and hydrogen purification", Journal of Membrane Science, 328(1-2), pp. 174–185, 2009.
https://doi.org/10.1016/j.memsci.2008.12.005

[28] Steel, K. M., Koros, W. J. "Investigation of porosity of carbon materials and related effects on gas separation properties", Carbon, 41(2), pp. 253–266, 2003.
https://doi.org/10.1016/S0008-6223(02)00309-3

[29] Hamm, J. B .S., Ambrosi, A., Griebeler, J. G., Marcilio, N. R., Tessaro, I. C., Pollo, L. D. "Recent advances in the development of supported carbon membranes for gas separation", International Journal of Hydrogen Energy, 42(39), pp. 24830–24845, 2017.
https://doi.org/10.1016/j.ijhydene.2017.08.071

[30] Gale, T. K., Bartholomew, C. H., Fletcher, T. H. "Decreases in the swelling and porosity of bituminous coals during devolatilization at high heating rates", Combustion and Flame, 100(1-2), pp. 94–100, 1995.
https://doi.org/10.1016/0010-2180(94)00071-Y

[31] Robeson, L. M. "The upper bound revisited", Journal of Membrane Science, 320(1-2), pp. 390–400, 2008.
https://doi.org/10.1016/j.memsci.2008.04.030